Removal of Cd^{2+} from Aqueous Solution by Nickel Oxide/CNT Nanocomposites

Navaei Diva, Tahereh; Zare, Karim
Department of Chemistry, Science and Research Branch, Islamic Azad University, Tehran, I.R. IRAN

Taleshi, Farshad*[+]
Department of Physics, Qaemshahr Branch, Islamic Azad University, Qaemshahr, I.R. IRAN

Yousefi, Mohammad
Department of Chemistry, Science and Research Branch, Islamic Azad University, Tehran, I.R. IRAN

ABSTRACT: *The present work investigates the efficiency of the nickel oxide/carbon nanotube (NiO/CNT) nanocomposite for the removal of Cd^{2+} metal ions from an aqueous. The NiO/CNT nanocomposite was synthesized by the direct co-precipitation method in an aqueous media in the presence of CNTs. The resulting materials were characterized by FTIR, XRD, SEM, N2 adsorption–desorption analysis. In order to optimize the adsorption of Cd^{2+} ions on NiO/CNT nanocomposite, the effects of the different parameters—namely pH, contact time, initial concentration of Cd^{2+}, and adsorbent dosage—were also studied. Experimental data revealed that the Cd^{2+} ions adsorption of the NiO/CNT nanocomposite was through Langmuir and Temkin isotherm models rather than the Freundlich model. The kinetic data of adsorption of Cd^{2+} ions on the adsorbent was best described by a pseudo-second-order equation, indicating their chemical adsorption. Thermodynamic parameters such as $\Delta G°$, $\Delta H°$, and $\Delta S°$ were calculated. The obtained values showed that the adsorption was spontaneous and exothermic in nature. The reusability test showed that the Cd^{2+} could be easily removed from the surface site of NiO/CNT nanocomposite by a 0.1 M nitric acid solution as the adsorption capacity was maintained after 5 cycles of the adsorption/desorption process. This suggests that NiO/CNT nanocomposite can be reused through many cycles of water treatment and regeneration.*

KEYWORDS: *Adsorption; Carbon nanotubes; Composite; Heavy metals; Removal*.

INTRODUCTION

The removal of Cadmium has attracted much attention from environmentalists as one of the most toxic and non-biodegradable heavy metals, which has detrimental effects on the environment and human health. There are various ways in which cadmium gets released into the environment through waste streams, including

***** *To whom correspondence should be addressed.*
+ E-mail: taleshi55@gmail.com
1021-9986/2019/1/141-154 *14/$/6.04*

the combustion of fossil fuels, metal production, application of phosphate fertilizers, electroplating, and the manufacturing of batteries, pigments, and screens [1, 2]. Even at small concentrations, cadmium may affect vital body organs like kidney, liver, lung, and cardiovascular, immunity, and reproductive systems [3]. According to the guidelines of the World Health Organization (WHO), the acceptable Cadmium concentration in drinking water is 0.005 mg/L [4]. Therefore, it is necessary to remove cadmium from water resources and industrial wastewater.

Different procedures such as filtration, chemical precipitation, coagulation, solvent extraction, electrolysis, ion exchange, membrane process, and adsorption have been reported as methods of separation, removal, and control of heavy metals [5–9]. Adsorption has been developed as one of the best methods for removal of heavy metals from water because it is cost-effective, easy to operate, and highly efficient. A variety of adsorbents such as clays, zeolites, dried plant parts, agricultural waste biomass, biopolymers, metal oxides, microorganisms, sewage sludge, fly ash, and activated carbon have been successfully utilized to remove cadmium ions from aqueous solutions [10–21].

Owing to their large specific surface area and small, hollow, and layered structure, multiwall carbon nanotubes have exhibited great potential as attractive adsorbents in wastewater treatment. Consequently, they can be easily modified by chemical treatment to increase their adsorption capacities [22]. The uses of MWCNTs as support for metallic oxides leads to the formation of highly efficient MO/MWCNT nanocomposites with higher sorption capacities, larger surface areas, and supported metallic oxides with better orientation degrees regarding net metallic oxides [23].

The present work aims to investigate the adsorption behavior of NiO-supported multiwall carbon nanotubes for the treatment of cadmium aqueous solutions. For this purpose, NiO/MWCNT composites were synthesized and characterized. The effect of experimental parameters, including pH, contact time, adsorbent dosage, and initial concentration of Cd^{2+} on adsorption, uptake was investigated. Moreover, the isotherm, kinetic, and thermodynamic aspects of the Cd^{2+} adsorption onto the NiO/MWCNT nanocomposite were also investigated [24].

EXPERIMENTAL SECTION

Materials

Nickel chloride hexa-hydrate ($NiCl_2.6H_{2O}$), sodium hydroxide (NaOH), CNTs (MWCNTs, US4309, purity>95%, 20 nm<d<30 nm), sulfuric, nitric and hydrochloric acids were utilized without further purification. Cadmium nitrate ($Cd(NO_3)_2$) was used to prepare Cd(II) stock solutions of 1000 mg/L. Cadmium solutions of different initial concentrations were prepared by diluting the stock solution for the desired concentrations.

Synthesis of NiO/CNT nanocomposite

NiO/CNT nanocomposite with 1:0, 2:1, 1:1, and 1:2 mol ratio was synthesized according to the previous study [25]. briefly, the surface of CNTs was functionalized as follows: initially, the desired amount of CNTs was added to the mixture of sulfuric/nitric/hydrochloric acids (6M) and ultrasonicated for 30 minutes. The obtained mixture was stirred for two hours at the temperature of 80 °C and was then filtered and washed with deionized water until the pH reached 7. Finally, the functionalized CNTs were dried in an oven at 120 °C.

For NiO/CNT nanocomposite preparation with 1:1 mol ratio, 3.2 g of $NiCl_2.6H_2O$ was dissolved in 50 mL deionized water containing 1 g of functionalized CNTs, ultrasonicated for 10 min and then magnetically stirred for 15 minutes at 80 °C. Addition of the known amount of NaOH solution to the mixture and stirring for 30 minutes completed the precipitation of $Ni(OH)_2$/CNTs nanocomposite. The obtained black slurry was filtered, washed with absolute ethanol and deionized water, dried at 120 °C for 24 h and finally calcinated at 300 °C for 2h.

Characterization techniques

The residual concentration of Cd^{2+} ions in the aqueous media was analyzed with the aid of Buck Scientific's 210 VGP flame atomic adsorption spectroscopy. The crystallinity of samples was revealed using Xpertpro Pananalytical, X-ray diffraction apparatus (Holland) with Cu(K_α) sources, and the wavelength of λ= 1.5405 Å. The morphology of powders was recorded using field emission scanning electron microscopy on the Mira3-XMU system. In addition, the presence of functional groups on the surface of CNTs was confirmed by WGF-510 Fourier transform infrared spectroscopy. The BET specific surface area and porosity were determined using

nitrogen adsorption–desorption porosimetry (77 K) by a porosimeter (Bel Japan, Inc.).

Adsorption experiments

As much as 0.1 g of NiO/CNT (1:1 mol ratio) was added to 50 mL of the solution containing Cd^{2+} metal ions and then stirred. After adsorption, the nanocomposite was separated from the solution, and the residual Cd^{2+} ion concentration was measured using flame atomic adsorption spectroscopy. The effect of different parameters, including pH, initial Cd^{2+}concentration, adsorbent dosage, and contact time on the amount of adsorption was investigated through the removal of the percentage (R) and adsorption capacity (q_e) of Cd^{2+} using the following expressions:

$$\%R = \frac{C_0 - C_e}{C_0} \times 100$$

$$q_e = \frac{C_0 - C_e}{C_0} \times V$$

Where C_0 and C_e are the initial and equilibrium concentrations of Cd^{2+} ions (mg/L), respectively, q_e is the equilibrium adsorption capacity of adsorbent in mg (metal ions)/g (adsorbent), m is the mass of the composite (g), and V is the volume of solution (L).

Reusability of nanocomposite

To test the reusability of the nanocomposite, the NiO/CNT nanocomposite containing Cd(II) was washed with HNO3 solution (0.1M). The resulting mixture was stirred at ambient temperature for 2 hours. After that, NiO/CNT nanocomposite was thoroughly washed with deionized water. After desorption, the nanocomposite was separated from the solution, and the residual Cd^{2+} ion concentration was measured using flame atomic adsorption spectroscopy. Then, the nanocomposite was re-used for the subsequent adsorption cycle. Five cycles of consecutive adsorption–desorption–regeneration were carried out to validate the reusability of NiO/CNT nanocomposite for the removal and recovery of Cd(II).

RESULT AND DISCUSSION

NiO/CNT Characterization

Fig. 1 indicates the X-ray diffraction pattern of the NiO/CNT nanocomposite with 1/0, 2:1, 1:1, and 1:2 mol ratio of NiO to CNT, respectively. Characteristic peaks at 2θ= 37.3˚ ,43.4˚, 62.9˚ and 75.4˚ are assigned to (111),

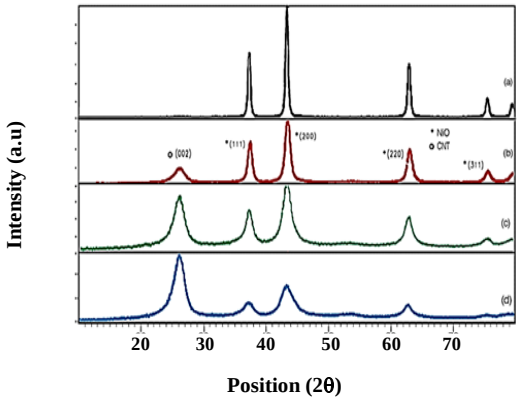

Fig. 1: XRD pattern of NiO/CNT nanocomposite with different mole ratios of NiO to CNTs, (a) 1:0, (b) 2:1, (c) 1:1, (d) 1:2

(200), (220), and (311) crystallographic orientations in NiO nanoparticles, accompanied by 2Θ=26 ˚ reflected from (002) plane in CNTs [26]. The size of NiO nanoparticles was calculated using the scherrer equation $(D = k\lambda/\beta\cos\theta)$. The main reflection peak of the XRD pattern at 2Θ=43˚ can be attributed to (200) plane. The size of NiO nanoparticles on CNT surface for mol ratio of 1:0, 2:1, 1:1, and 1:2 were determinate 28.3, 21.29, 18.5, and 7.4 nm, respectively. The morphology of NiO/CNT and pure NiO was analyzed using FESEM images shown in Fig. 2. It is well known that after the functionalization of MWCNTs, their surface indicates polar groups, such as carboxyl or hydroxyl groups, which can interact through hydrogen bonding with the NiO surface. It can be seen in Fig.2a that NiO nano-crystallites are aggregated together, forming clusters with larger grains. The formation of this agglomerated structure has unfavorable effects on the physical and chemical properties of nanoparticles. The use of CNTs as a support material for the growth of nanoparticles reduces the agglomeration and changes the powder morphology from a cluster-like to a filamentous structure (Fig.2b). It is observed that the nanoparticles on the surface of the CNTs possess smaller dimensions than pure NiO nanoparticles. This result is confirmed using the data obtained from XRD diagrams.

N_2 adsorption-desorption isotherms are performed to investigate the specific surface area, mean pore diameter and the total pore volume of NiO/CNT nanocomposite (Fig. 3). The specific surface area, mean pore diameter and the total pore volume of NiO/CNT nanocomposite

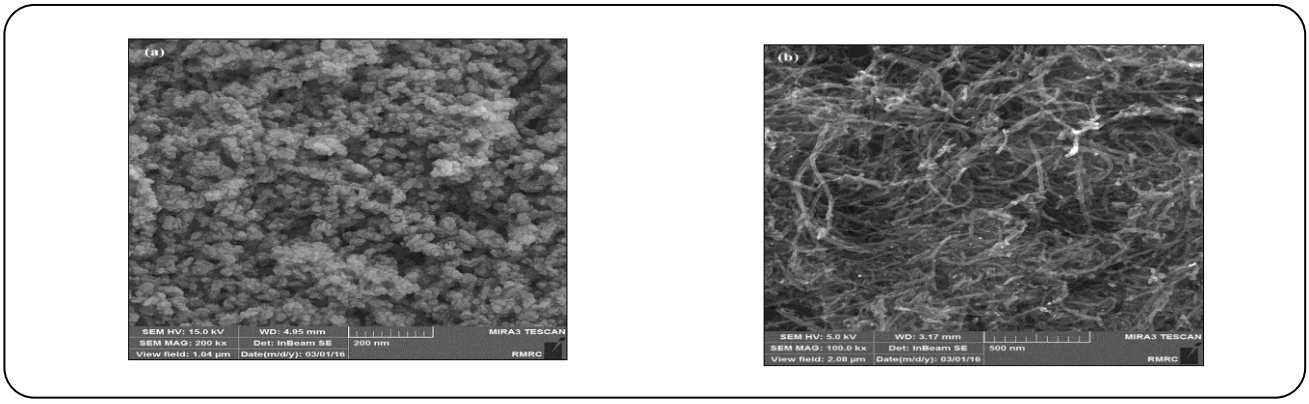

Fig. 2: FESEM of (a) pure NiO and (b) NiO/CNT nanocomposite.

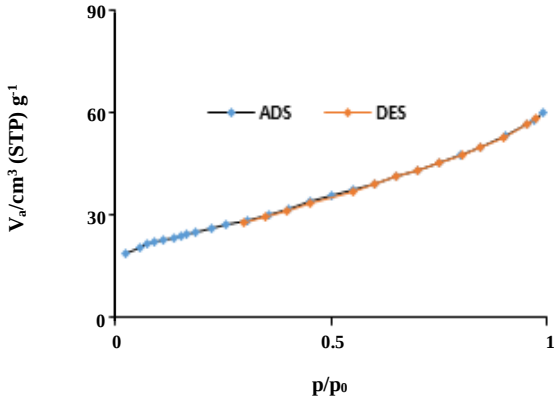

Fig. 3: N_2 isothermal adsorption and desorption profiles.

is determined to be 90 m^2/g, 4.16 nm, and 9.26×10^{-2} cm^3/g, respectively. Fig. 4 indicates schematic illustration of the various steps involved to obtain the absorbent.

In order to determine the type of chemical bonds formed on the surface of CNTs and nanocomposite after functionalization, FT-IR spectra of samples were recorded. Fig. 5 illustrates FT-IR spectra of oxidized and raw MWCNTs. According to the spectra, peaks located at 420 cm^{-1} are attributed to the vibrations of Ni-O bond, 1220 cm^{-1}due to the existence of C-O groups, and 1519 cm^{-1} is related to the stretching vibrations of C=C, 1739 cm^{-1} to C=O bond and 3446 cm^{-1} to O-H groups.

Batch adsorption experiments

Effect of pH

To investigate the effect of pH, the initial pH of the solutions varied from 3 to 8, and not more than 8, to avoid cadmium precipitation. Fig. 6 indicates the effect of pH on the removal of cadmium ions by the NiO/CNT nanocomposite. It can be observed that the removal percentage increases sharply with a rise of pH from 3 to 6, while it maintains its level with increasing pH values at pH 6 to 8 and reaches its maximum. It is known that cadmium species is present in the form of Cd^{2+}, $Cd(OH)^+$, $Cd(OH)_2^0$, and $Cd(OH)_3^-$ at different pH values [27]. It has been reported that at pH<9, the predominant cadmium specie is Cd^{2+}, and the removal of Cd^{2+} is mainly accomplished by adsorption reaction. However, at pH>9, cadmium ions precipitate because of the high concentration of OH^- ions in the solution. Therefore, the lower adsorption percentage of Cd^{2+} on NiO/CNT at low pH can be attributed partly to the competition between H^+ and Cd^{2+} ions on the surface sites. As the pH value is higher, the negative surface charge on NiO/CNT increased due to deprotonation of functional groups on the adsorbent, causing electrostatics attraction between negative sites on the adsorbent and Cd^{2+} ions. This results in higher adsorption of metal ions. Hence, the solution pH of 7 could be an optimum value for the Cd(II) ion removal application of the NiO/CNT nanocomposite.

Effect of adsorbent dosage

The effect of the adsorbent dosage on the removal percentage for the 20 ppm solution of Cd^{2+} by the NiO/CNT nanocomposite and CNTs is shown in Fig. 7. In both adsorbents, the percentages of adsorbed cadmium increased as the adsorbent dosage was increased over the range of 0.01–0.1 g. Removal of approximately 97% was achieved when 0.1 g of the NiO/CNT nanocomposite was soaked in 50mL of the 20 ppm Cadmium solution compared with a 37% removal when 0.1g of CNTs was used. Based on the mentioned results, it is obvious

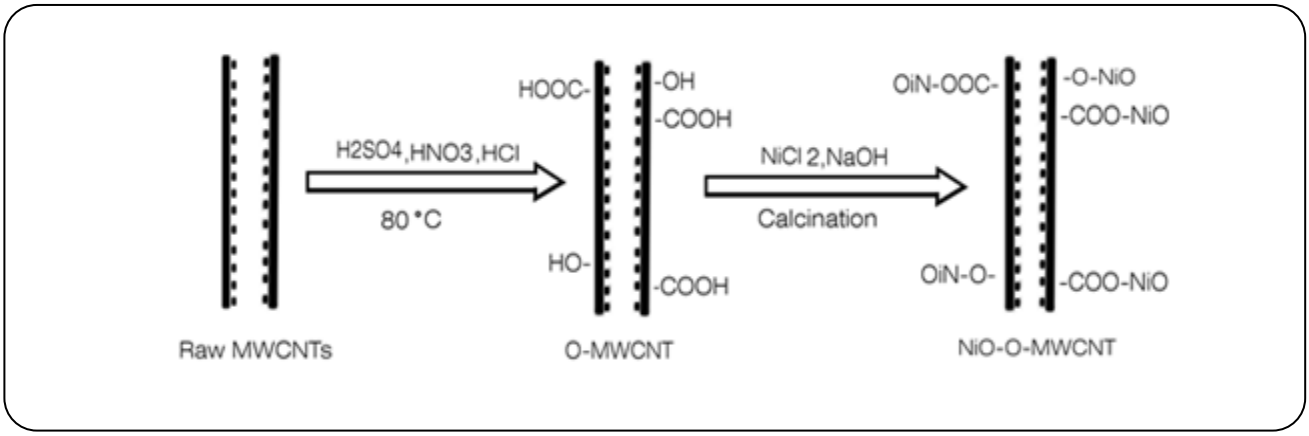

Fig. 4: Schematic illustration of the various steps involved to obtain the absorbent.

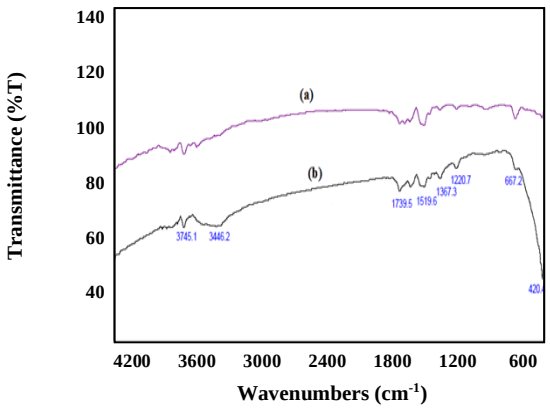

Fig. 5: FT-IR of (a) CNTs, (b) NiO/CNT.

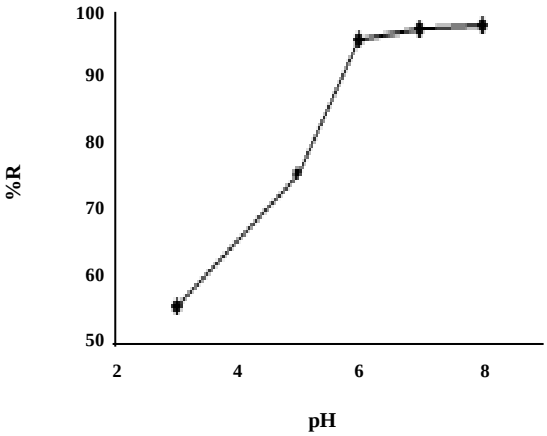

Fig. 6: Effect of solution pH on Cd^{2+} removal by NiO/CNT nanocomposite (initial concentration 10 mg, 0.2 g NiO/CNT /50 mL solution, initial pH of solution 7, contact time 15 min, temp 298 K).

that the mechanism of nanocomposite adsorption toward Cd^{2+} was perhaps derived from three reasons. One reason might be based on van der Waals interactions between the positively charged cadmium ions and the hexagonally arrayed carbon atoms in graphite sheets of the CNTs. The second one might be due to the electrostatic attraction between Cd^{2+} cations and the negatively charged CNTs' adsorbent surface. The third one might be attributed to the electrostatic attraction between the pairs of electrons on the oxygen atoms of nickel oxide and Cd^{2+} ions [24, 28].

Effect of Cd^{2+} initial concentration

The variation in the removal percentage with initial concentrations of Cd^{2+}ions is shown in Fig. 8. It is evident that increasing the Cd^{2+} initial concentration from 2 ppm to 25 ppm reduces the removal efficiency from almost 97% to 78%. At lower Cd^{2+} initial concentrations, adequate amounts of active sites are available for adsorption, leading to a higher adsorption capacity; at higher initial Cd^{2+} concentrations, the amount of metal ions is higher compared to active adsorption sites and therefore the removal efficiency decreases [28].

Adsorption kinetics

The effect of contact time on the removal percentage of Cd^{2+} using NiO/CNT is depicted in Fig.9a. The highest amount of adsorption was achieved after 15 minutes of adsorption, which was approximately 99%. Therefore, 15 minutes was considered as the optimum contact time for Cd^{2+} adsorption on the NiO/CNT nanocomposite.

To investigate the mechanism of cadmium adsorption, adsorption kinetic constants and potential rate controlling

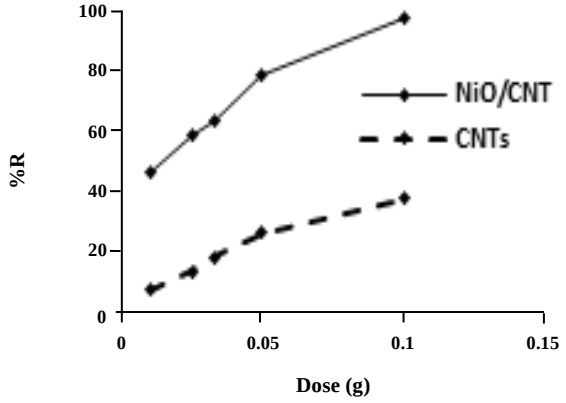

Fig. 7: Effect of adsorbent dose on Cd^{2+} removal by NiO/CNT nanocomposite (initial concentration 20 mg/L, initial pH of solution 7, contact time 15 min, temp 298 K).

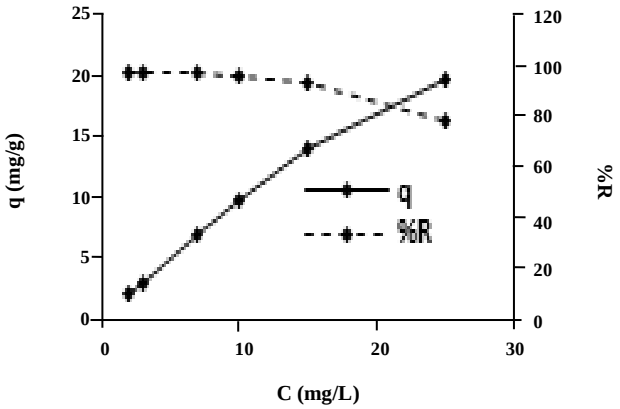

Fig. 8: Effect of initial Concentration on Cd^{2+} removal by NiO/CNT nanocomposite (contact time 15 min., 0.05 g NiO/CNT /50 mL solution, initial pH of solution 7, temp., 298 K).

steps, and different kinetic models, such as Lagergren pseudo first-order, Ho pseudo second-order [29], and intra-particle diffusion rate equations were applied to fit the experimental data.

The pseudo first-order rate equation is:

$$Ln(q_e - q_t) = Lnq_e - k_1 t$$

Where q_e and q_t (mg/g) are the adsorption capacities at equilibrium and at time t(min), respectively, and k_1 is the pseudo first-order rate constant (min^{-1}).

The pseudo second-order rate equation is:

$$\frac{t}{q_t} = \frac{1}{k_Z q_e^2} + \frac{1}{q_e} t$$

$$h = k_2 q_e^2$$

Where k_2 is the pseudo second-order rate constant (g/mg min) and h is the initial adsorption rate (mg/g min) [30].

The model parameters, such as model constants, equilibrium adsorption capacity, and the value of the correlation coefficients (R^2) are depicted in Figs. 9b and 9c and Table 1.

According to Table 1, it can be seen that the adsorption of Cd^{2+} on the NiO/CNT nanocomposite can best be described by the pseudo second-order model with higher values of the correlation coefficient (R^2) and closer values of the calculated adsorption capacity ($q_{e,cal}$) to the experimental one ($q_{e,exp}$). It means that the adsorption of Cd^{2+} onto NiO/CNT may be the chemisorption involving valence forces by sharing or exchanging electrons between cadmium ions and nanocomposite [31].

The intra-particle diffusion equation is:

$$q_t = K_{int} t^{1/2} + C_{int}$$

where k_{int} is the intra-particle diffusion rate constant (mg g^{-1} $min^{1/2}$) and C_{int} is a constant related to the thickness of the boundary layer.

According to the intra-particle diffusion mode, if the plot of q_t versus $t^{1/2}$ is linear and passes through the origin, the intra-particle diffusion is the only rate-limiting step. Fig. 9d shows three straight lines with different slopes and intercepts values in which larger values of intercepts (C) are related to cases where surface diffusion has a greater role as the rate-limiting step. [32]. The first line depicts the instantaneous adsorption or external surface adsorption stage; the second line represents the intra-particle diffusion; and finally, the third linear portion shows the final equilibrium stage and the saturation of the adsorbent surface. Owing to an extremely low Cd^{2+} concentration in the solution, intra-particle diffusion starts to slow down. The K_{int} and C values of each line are shown in Table 2. The results of the observation confirm both intra-particle diffusion and surface adsorption mechanism. Further results indicate $k_1 > k_2 > k_3$ due to the fact that the concentration of Cd^{2+} left in the solutions gradually decreases.

Adsorption isotherms

The adsorption isotherm represents the adsorption capacity at different aqueous equilibrium concentrations.

Table 1: Adsorption Kinetic Parameters of Cd^{2+} Adsorption on NiO/CNT.

Model	Psedo-first-order		Psedo-second-order	
$q_{e,exp}$ (mgg^{-1})	$K_1(min^{-1})$	0.16920	K_2(g $mg^{-1}min^{-1}$)	0.97
2.5	$q_{e,cal}$(g $mg^{-1}min^{-1}$)	0.39	$q_{e\,cal}$(mg g^{-1})	2.54
	0.865	R^2	h(mgg^{-1} min^{-1})	6.26
			R^2	0.9998

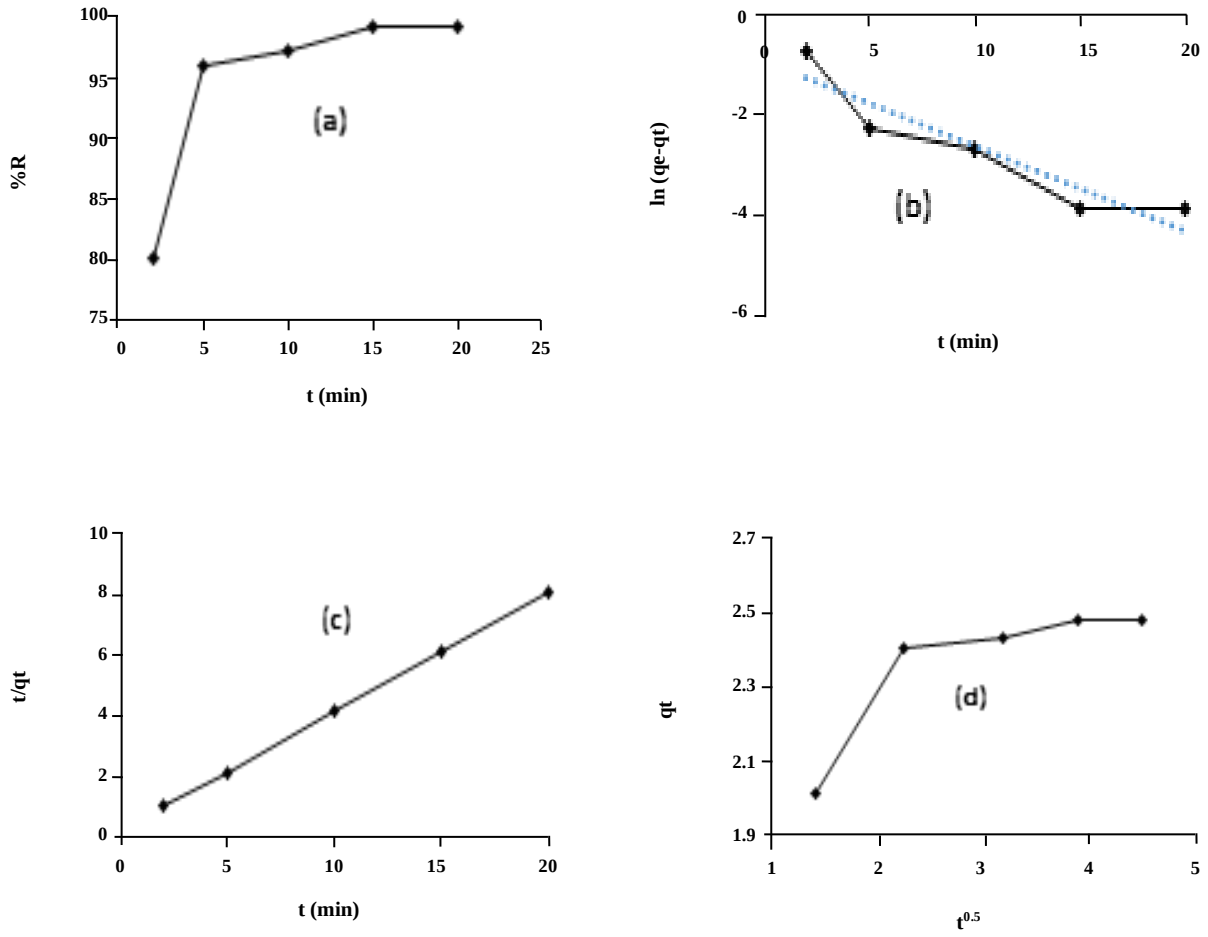

Fig. 9: (a) Effect of contact time (initial concentration 10 mg/L, 0.2 g NiO/CNT /50 mL solution, initial pH of solution 7, temp., 298 K), (b) pseudo-first-order, (c) pseudo-second-order, and (d) intra particle diffusion kinetic models for Cd^{2+}

Equilibrium data provide information about the capacity of the adsorbent or the amount required for removing a unit mass of metal ions under the system conditions. Four adsorption isotherms were employed to model the adsorption of cadmium ions on the NiO/CNT nanocomposite, namely Langmuir, Freundlich, Temkin, and Dubinin–Radushkevich (D-R) equilibrium isotherm models.

The Langmuir isotherm can be successfully applied for describing the monolayer adsorption phenomena with the following equation [27]:

$$\frac{1}{q_e} = \left(\frac{1}{q_m K_L}\right)\left(\frac{1}{C_e}\right) + \frac{1}{q_m}$$

Where q_m is the maximum adsorption capacity of

Table 2: Intra particle diffusion rate parameters for adsorption of Cd^{2+} on NiO/CNT.

Rate controlling step	K_{int} (g/mg $min^{0.5}$)	C_i	R^2
1	0.4699	1.3475	1
2	0.0483	2.2875	0.9534
3	0.0167	2.4155	1

Table 3: R_L values for different Cd^{2+} ions concentrations.

Initial Cd^{2+} concentrations (mg/L)	2	3	7	10	15	25
R_L	0.222	0.160	0.075	0.054	0.037	0.022

the adsorbent (mg/g) and K_L is the Langmuir constant (L/mg). The values of q_m and K_L are obtained graphically from the $(1/q_e)$ versus $(1/C_e)$ plot, which yields to a straight line with the slope of $(1/q_m K_L)$ and intercept of $(1/q_m)$.

The essential features of the Langmuir isotherm can be expressed in terms of the separation factor R_L defined by [33, 34]:

$$R = \frac{1}{1 + KL.C0}$$

Where C_0 is the initial Cd^{2+} ion concentration (mg/L). The R_L value indicates the adsorption nature to be irreversible (R_L =0), favorable (0 < R_L< 1), linear (R_L = 1), or unfavorable (R_L> 1). In the present study, the values of R_L (Table 3) were found to be within the range of 0–1, thus indicating that the adsorption process is favorable.

The Freundlich isotherm provides a relation between the number of metal ions adsorbed per unit mass of the adsorbent (q_e) and the concentration of the ion at equilibrium (C_e) with the following representation [35]:

$$\text{Log}\, q_e = \log K_F + \frac{1}{n}\text{Log}\, C_e$$

Where n and K_F are Freundlich constants. The values of n and K_F are also achieved graphically by plotting Log q_e versus Log C_e, which result in a straight line with the slope of 1/n and intercept of Log K_F.

The Temkin isotherm assumes that the heat of adsorption in any adsorption system most often decreases because of the interaction between the absorbent and the adsorbent [27, 36]. The Temkin isotherm is derived from the following equation:

$$q = B_T \text{Ln}(K_T) + B_T \text{Ln}(C_e)$$

$$B_T = \frac{RT}{b}$$

Where K_T is the Temkin isotherm equilibrium constant (L/mg), b_T is Temkin isotherm constant (J/mol), R is the universal gas constant (8.314 J/mol K), T is the temperature at 298 K, and B_T is the constant related to the heat of adsorption.

The linear form of Dubinin–RadushKevich (D-R) isotherm usually is utilized to distinguish the physical and chemical nature of the adsorption on heterogeneous surfaces with the following equation [37]:

$$\ln qe = \ln Q_s - B\varepsilon^2$$

Where Qs is the theoretical monolayer saturation capacity (mg/g), B is the (D-R) model constant (mol^2/kJ). ε, is the polanyi potential, which is equal to:

$$\varepsilon = RT \ln\left(1 + \frac{1}{Ce}\right)$$

The mean energy of sorption E (kJ/mol) is related to B as:

$$E = \frac{1}{\sqrt{2B}}$$

The plot of ln q_e vs. ε^2 is presented in Fig 10d. The constants obtained for D–R isotherms are shown in Table 4. The adsorption energy (E) gives information about chemical and physical nature of adsorption. It was found

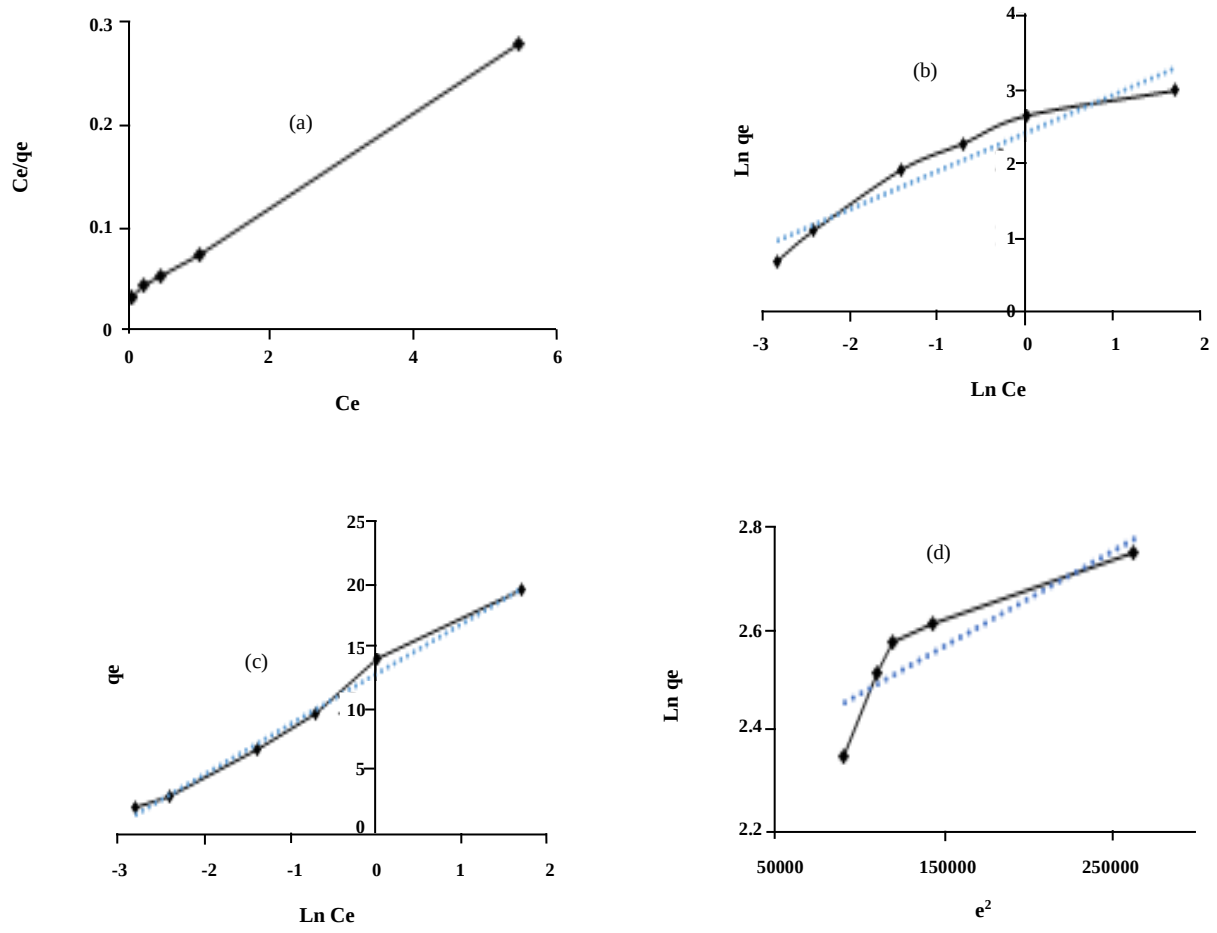

Fig. 10: (a) Langmuir, (b) Freundlich, (c) Temkin, and (d) (D-R) adsorption isotherm for Cd^{2+} removal on NiO/CNT nanocomposite.

to be 0.5 kJ/mol, which is in the range of physical adsorption reactions. Fig. 10 illustrates Langmuir (10a), Freundlich (10b), and Temkin (10c) for the adsorption of Cd^{2+} on the NiO/CNT nanocomposite, respectively, with the obtained parameters summarized in Table 4. It can be seen that Langmuir and Temkin models simulate the experimental data better than the Freundlich model.

To get the synthesized absorbent efficiency approved, its maximum amount of absorption was compared with other adsorbents. As shown in Table 5 the maximum absorption capacity obtained in this study is a significant comparison with other adsorbents, which indicates the efficiency of the synthetic adsorbent.

Adsorption thermodynamics

The effect of temperature on the adsorption of Cd^{2+} ions by NiO/CNT was investigated at 25, 35, 45, 55, and 75 °C. The thermodynamic parameters, free energy change (ΔG°, enthalpy change (ΔH°), and entropy change (Δ∑°) were calculated to evaluate the thermodynamic feasibility and spontaneous nature of the process. The thermodynamic parameters and K_d values can be obtained from Van't Hoff equations [46]:

$$\Delta G^\circ = -RT \ln K_d$$

$$K_d = \frac{q_e}{C_e}$$

$$\ln K_d = \frac{\Delta S^\circ}{R} - \frac{\Delta H^\circ}{RT}$$

Where K_d is the distribution coefficient, T is the temperature (K), R is the universal gas constant (8.3145 J/mol K), C_e is the equilibrium concentration

Table 4: Adsorption isotherm Parameters of Cd^{2+} Adsorption on NiO/CNT.

Isotherm model	Parameter		
Langmuir	K_L	L/mg	1.75
	q_m	mg/g	21.74
	R^2		0.9996
Freundlich	K_F	mg/g	10.96
	1/n		0.5197
	R^2		0.9181
Temkin	K_T	L/mg	23.81
	B_T	mg/g	4.0497
	R^2		0.9917
(D-R)	Q_s	mg/g	9.8
	$B\times10^{-6}$	Mol^2/KJ^2	2.0
	E	KJ/mol	0.5
	R^2		0.7792

Table 5: The equilibrium capacities of Cd^{2+} on various adsorbents.

Adsorbents	q_{max} (mg/g)	References
Saxaul Tree Ash	2.65	[38]
Bagasse Fly Ash	14	[39]
MWCNTs(H2O2)	2.6	[40]
MWCNTs (HNO3)	5.1	
MWCNTs(KMNO4)	11	
MWCNTs grown on Al2O3	8.89	[41]
MWCNTs (HNO3)	7.42	[42]
Ethylenediamine functionalized MWCNTs	25.7	[43]
Alumina/MWCNTs	27.21	[44]
Nitrogen doped CNTs	31	[45]
NiO/CNTs	21.74	This study

in the aqueous phase (mg/L), and q_e is the amount of Cd^{2+} adsorbed per unit mass of the adsorbent (mg/g). The effects of the temperature and Van't Hoff plot have been depicted in Fig. 11. The results of the calculation are presented in Table 6. The negative value of ΔG° indicates that the adsorption reaction was spontaneous. The negative values of ΔH° and ΔS° are attributed to the exothermic nature of adsorption as well as to an increase in temperature that caused the desorption of Cd^{2+} ions on the NiO/CNT nanocomposite.

Reusability of nanocomposite

Fig. 12 shows the removal efficiency of Cd(II), during five cycles of adsorption–desorption–regeneration, from a 50mL solution of initial Cd(II) concentration 20 mg/L. As can be seen, no significant decrease in the adsorption capacity of NiO/CNT nanocomposite during the five cycles was observed. The results demonstrated that NiO/CNT nanocomposite can be used for the removal and recovery of metal ions from wastewater over a number of cycles, indicating its suitability for the design of a continuous process.

Table 6: Values of Thermodynamic Parameters of Adsorption of Cd^{2+} on NiO/CNT.

ΔS°	ΔH°	ΔG°(temperature, K)				
–55.48	–19.49	–3.12(298)	–2.28(308)	–1.67(318)	–1.25(328)	–0.29(348)

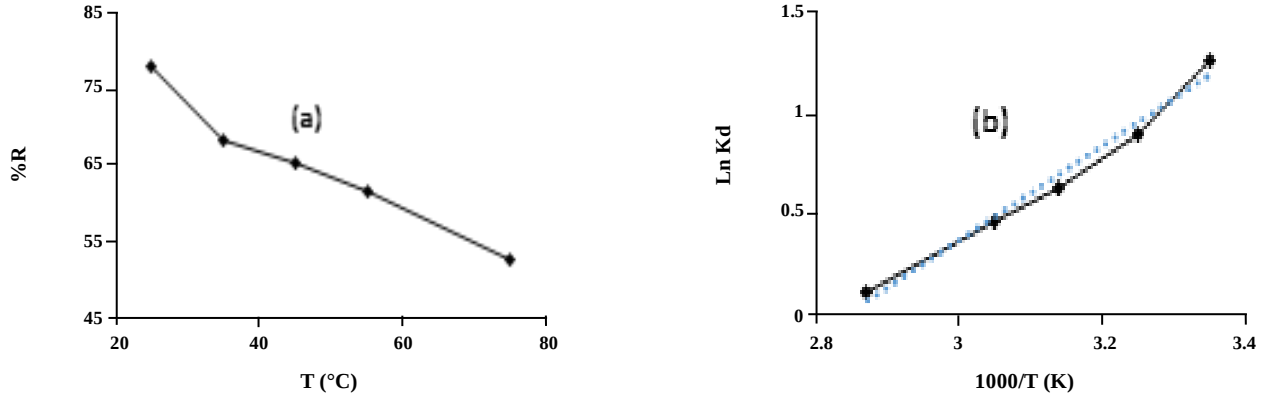

Fig. 11: (a) The effect of temperature, and (b) Van't Hoff plot of Ln K_d versus 1/T for Cd^{2+} removal on NiO/CNT nanocomposite.

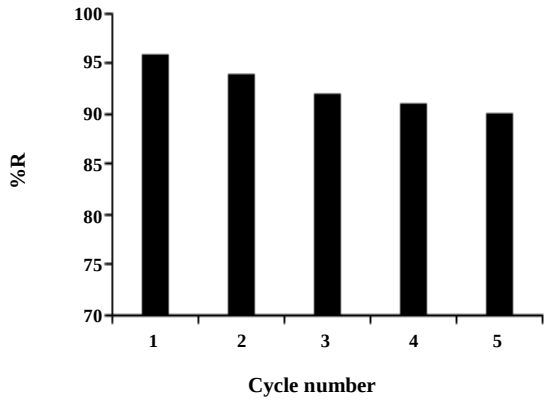

Fig. 12: Reusability of NiO/CNT nanocomposite for adsorption/desorption of Cd(II) during five cycles. Adsorption: initial concentration of Cd(II): 20mg/L, adsorbent dose: 0.05 g, contact time: 2 h, T = 298 K. Desorption: HNO_3, 0.1 M.

CONCLUSIONS

In this study, the NiO/CNT nanocomposite has been synthesized by a direct co-precipitation method. This study has shown that the NiO/CNT nanocomposite is ideal for the adsorption of Cd^{2+} metal ions from the aqueous solution. The kinetic study of Cd^{2+} ions on the NiO/CNT nanocomposite has also been performed on the basis of pseudo first-order, pseudo second-order, and intra-particle models. The results revealed that the adsorption kinetics have been described best by the pseudo second-order equation, thus suggesting that chemical interaction controls the adsorption process [26]. The experimental data are more consistent with both Langmuir and Temkin isotherm models than with the Freundlich model. Thermodynamic studies have shown that the adsorption of Cd^{2+} on the NiO/CNT nanocomposite has an exothermic and spontaneous nature. The Reusability test showed that CNTs could be efficiently regenerated by a 0.1 M HNO3 solution as the adsorption capacity was maintained after 5 cycles of the adsorption/desorption process. This suggests that NiO/CNT nanocomposite can be reused through many cycles of water treatment and regeneration for the removal of Cd^{2+} from aqueous solution.

Acknowledgment

The authors would like to acknowledge the support provided by Islamic Azad University, Science and Research Branch and Savadkooh Branch for their contribution to the publication of this paper.

Received : Jun. 6, 2017 ; Accepted : Feb. 5, 2018

REFERENCES

[1] Sharma Y.C., Thermodynamics of Removal of Cadmium by Adsorption on an Indigenous Clay, *Chem. Eng. J.*, **145**: 64–68 (2008).

[2] Perez-Marin A.B., Zapata V.M., Ortuno J.F., Aguilar M., Saez J., Llorens M., Removal of Cadmium from Aqueous Solutions by Adsorption onto Orange Waste, *J. Hazard. Mater.*, **139**: 122–131 (2007).

[3] Flowler B.A., Monitoring of Human Populations for Early Markets of Cadmium Toxicity, A Review, *Toxicol. Appl pharmacol*., **238**(3): 294-300 (2009).

[4] Wang F.Y., Wang H., Ma J.W., Adsorption of Cadmium (II) Ions from Aqueous Solution by a New Low-Cost Adsorbent—Bamboo Charcoal, *J. Hazard. Mater*., **177**(1): 300-306 (2010).

[5] Poorsadeghi S., Kassaee M.Z., Fakhri H., Mirabedini M., Removal of Arsenic from Water Using Aluminum Nanoparticles Synthesized through Arc Discharge Method, *Iran. J. Chem. Chem. Eng. (IJCCE)*, **36**(4): 91-99 (2017).

[6] Saffaj N., Loukil H., Younssi S.A., Albizane A., Bouhria M., Persin M., Larbot A., Filtration of Solution Containing Heavy Metals and Dyes by Means of Ultrafiltration Membranes Deposited on Support Made of Morrocan Clay, *Desalination*, **168**: 301 (2004).

[7] Qdias H.A., Moussa H., Removal of Heavy Metals from the Wastewater by Membrane Processes: A Comparative Study, *Desalination*, **164**: 105-110 (2004).

[8] Shi Z., Zou P., Guo M., Yao S., Adsorption Equilibrium and Kinetics of Lead Ion onto Synthetic Ferrihydrites, *Iran. J. Chem. Chem. Eng.(IJCCE)*, **34**(3): 25-32 (2015).

[9] Chen G.H., Electrochemicals Technologies in Wastewater, *Sep. Purif. Technol*, **38**(10): 11 (2004).

[10] Sharma Y.C., Thermodynamics of Removal of Cadmium by Adsorption on an Indigenous Clay, *Chem. Eng. J.*, **145**: 64–68 (2008).

[11] Tan G.Q., Xiao D., Adsorption of Cadmium Ion from Aqueous Solution by Ground wheat Stems, *J. Hazard. Mater.*, **164**: 1359–1363 (2009).

[12] Benguella B., Benaissa H., Cadmium Removal from Aqueous Solutions by Chitin: Kinetic and Equilibrium Studies, *Water Res.*, **36**: 2463–2474 (2002).

[13] Meng Y.T., Zheng Y.M., Zhang L.M., He J.Z., Biogenic Mn Oxides for Effective Adsorption of Cd from Aquatic Environment, *Environ. Pollut*., **157**: 2577–2583 (2009).

[14] Soltani R.D.C., Jafari A.J., Khorramabadi Gh.S., Investigation of Cadmium (II) Ions Biosorption onto Pretreated Dried Activated Sludge, *Am. J. Environ. Sci.*, **5**: 41–46 (2009).

[15] Sanchooli Moghaddam M., Rahdar S., Taghavi M., Cadmium Removal from Aqueous Solutions Using Saxaul Tree Ash, *Iran. J. Chem. Chem. Eng. (IJCCE)*, **35** (3): 45-52 (2016).

[16] Haq Nawaz B., Rubina K., Muhammad Asif H., Biosorption of Pb(II) and Co(II) on Red Rose Waste Biomass, *Iran. J. Chem. Chem. Eng.(IJCCE)*, **30**(4): 81-88 (2011).

[17] Garg U., Kaur M.P., Jawa G.K., Sud D., Garg V.K., Removal of Cadmium (II) from Aqueous Solutions by Adsorption on Agricultural Waste Biomass, *J. Hazard. Mater*., **154**: 1149–1157 (2008).

[18] Semerjian L., Equilibrium and Kinetics of Cadmium Adsorption from Aqueous Solutions Using Untreated Pinus Halepensis Sawdust, *J. Hazard. Mater.*, **173**: 236–242 (2010).

[19] Li Z.Z., Katsumi T., Imaizumi S., Tang X.W., Inui T., Cd(II) Adsorption on Various Adsorbents Obtained from Charred Biomaterials, *J. Hazard. Mater.*, **183**: 410–420 (2010).

[20] Kumar R., Singh R.K., Dubey P.K., Singh D. P., Yadav R.M., Tiwari R.S., Freestanding 3D Graphene–Nickel Encapsulated Nitrogen-Rich Aligned Bamboo Like Carbon Nanotubes for High-Performance Supercapacitors with Robust Cycle Stability, *Adv. Mater. Interfaces*, **2**: 1500191 (2015).

[21] Tashauoei H.R., Attar H.M., Amin M.M., Kamali M., Nikaeen M., Dastjerdi M.V., Removal of Cadmium and Humic Acid from Aqueous Solutions Using Surface Modified Nanozeolite A, *Int. J. Environ. Sci. Technol.*, **7**: 497–508 (2010).

[22] Visa M., Bogatu C., Duta A., Simultaneous Adsorption of Dyes and Heavy Metals from Multicomponent Solutions Using Fly Ash, *Appl. Surf. Sci.*, **256**: 5486–5491 (2010).

[23] Chen C.L., Wang X.K., Nagatsu M., Europium Adsorption on Multiwall Carbon nanotube/Iron Oxide Magnetic Composite in the Presence of Polyacrylic Acid, *Environ. Sci. Technol.*, **43**: 2362–2367 (2009).

[24] Gupta V. K., Agarwal S., Saleh T. A., Synthesis and Characterization of Alumina-Coated Carbon Nanotubes and Their Application for Lead Removal, *J. Hazard. Mater*., **185**: 17-23 (2011).

[25] Navaei Diva T., Zare K., Taleshi F., Yousefi M., Synthesis, Characterization, and Application of Nickel Oxid/CNT Nanocomposites to Remove Pb^{2+} from Aqueous Solution, *J. Nanostruct. Chem.*, 7(3): 273-281 (2017).

[26] Taleshi F., A New Strategy for Increasing the Yield of Carbon Nanotubes by the CVD Method, *Fullerenes, Nanotubes, and Carbon Nanostructures*, **22:** 921-927 (2014).

[27] Pashai Gatabi M., Milani Moghaddam H., Ghorbani M., Efficient Removal of Cadmium Using Magnetic Multiwalled Carbon Nanotube Nanoadsorbents: Equilibrium, Kinetic, and Thermodynamic Study, *J. Nanopart Res*., **18**: 189 (2016).

[28] Rao M.M., Ramesh A., Rao G.P.C., Seshaiah K., Removal of Copper and Cadmium from the Aqueous Solutions by Activated Carbon Derived from Ceiba pentandra Hulls, *J. Hazard. Mater*., **B 129**: 123–129 (2006).

[29] Lu C., Chiu H., Liu C., Removal of Zinc(II) from Aqueous Solution by Purified Carbon Nanotubes: Kinetics and Equilibrium Studies, *Ind. Eng. Chem. Res*., **45**: 2850-2855 (2006).

[30] Kanthapazham R., Ayyavu C., Mahendiradas D., Removal of Pb^{2+}, Ni^{2+} and Cd^{2+} Ions in Aqueous Media Using Functionalized MWCNT Wrapped Polypyrrole Nanocomposite, *Desalination and Water Treatment*, **57**(36): 16871-16885 (2016).

[31] Gu H., Lou H., Tian J., Liu S., Tang Y., Reproducible Magnetic Carbon Nanocomposites Derived from Polystyrene with Superior Tetrabromobisphenol A Adsorption Performance, *J. Mater. Chem. A*, **4**: 10174-10185 (2016).

[32] Torabinejad A., Nasirizadeh N., Yazdanshenas M.E., Tayebi H.A., Synthesis of Conductive Polymer-Coated Mesoporous MCM-41 for Textile Dye Removal from Aqueous Media, *Journal of Nanostructure in Chemistry*, **7**(3): 217-229 (2017).

[33] Tahermansouri H., Mohamadian Ahi R., Kiani F., Kinetic, Equilibrium and Isotherm Studies of Cadmium Removal from Aqueous Solutions by Oxidized Multi-Walled Carbon Nanotubes and the Functionalized Ones with Thiosemicarbazide and Their Toxicity Investigations: A Comparison, *J. Chin. Chem. Soc*., **61**: 1188–1198 (2014).

[34] Tahermansouri H., Dehghan Z., kiani F., Phenol Adsorption from Aqueous Solutions by Functionalized Multiwalled Carbon Nanotubes with a Pyrazoline Derivative in the Presence of Ultrasound, *RSC. Adv.*, **5**: 44263–44273 (2015).

[35] Rengaraj S., Joo C.K., Kim Y., Yi J., Kinetics of Removal of Chromium from Water and Electronic Process Wastewater by Ion Exchange Resins: 1200H, 1500H and IRN97H., *J. Hazard. Mater*., **B 102**: 257–275 (2003).

[36] Faraji H., Mohamadi A. A., Soheil Arezomand H. R., Mahvi A. H., Kinetics and Equilibrium Studies of the Removal of Blue Basic 41 and Methylene Blue from Aqueous Solution Using Rice Stems, *Iran. J. Chem. Chem. Eng.(IJCCE)*, **34**(3): 33-42 (2015).

[37] Chen Y., Li F., Kinetic Study on Removal of Copper(II) Using Goethite and Hematite Nano-Photo Catalysts, *J. Coloid and Interface Science*, **347**: 277-281(2010).

[38] Sanchooli Moghaddam M., Rahdar S., Taghavi M., Cadmium Removal from Aqueous Solutions Using Saxaul Tree Ash, *Iran. J. Chem. Chem. Eng. (IJCCE)*, **35**(3): 45-52 (2016).

[39]Gupta V.K., Jain C., Ali I., Sharma M., Saini V., Removal of Cadmium and Nickel from Wastewater Using Bagasse Fly Ash—A Sugar Industry Waste, *Water Res*., **37**(16): 4038-4044 (2003).

[40] Li Y.H., Wang S., Luan Z., Ding J., Xu C., Wu D., Adsorption of Cadmium (II) from Aqueous Solution by Surface Oxidized Carbon Nanotubes, *Carbon*, **41**: 1057–1062 (2003).

[41] Hsieh S.H., Horng J.J., Adsorption behavior of Heavy Metal Ions by Carbon Nanotubes Grown on Microsized Al_2O_3 Particles, *Int. J. Miner Metal Mater*., **14**: 77–84 (2007).

[42] Liang P., Liu Y., Guo L., Zeng J., Lu H., Multi Walled Carbon Nanotubes as Solid-Phase Extraction Adsorbent for the Preconcentration of Trace Metal Ions and Their Determination by Inductively Coupled Plasma Atomic EmissionSspectrometry, *J. Anal. at Spectrom.*, **19**:1489–1492 (2004).

[43] Vukovic´ G.D., Marinkovic´ A..D, olic´ M., Ristic´ M.Đ., Aleksic´ R., Peric´-Grujic´ A.A., Uskokovic´ P.S., Removal of Cadmium from Aqueous Solutions by Oxidized and Ethylenediamine-Functionalized Multi-Walled Carbon Nanotubes, *Chem. Eng. J*., **157**: 238–248 (2010).

[44] Liang J., et al, Facile Synthesis of Alumina-Decorated Multi-Walled Carbon Nanotubes for Simultaneous Adsorption of Cadmium Ion and Trichloroethylene, *Chem. Eng. J.*, **273**:101–110 (2015).

[45] Andrade-Espinosa G., Mun˜oz-Sandoval E., Terrones M., Endo M., Terrones H., Rangel-Mendez J.R., Acid Modified Bamboo-Type Carbon Nanotubes and Cup-stacked-Type Carbon Nanofibres as Adsorbent Materials: Cadmium Removal from Aqueous Solution, *J. Chem. Technol. Biotechnol.*, **84**: 519–524 (2009).

[46] Gu H., Lou H., Ling D., Xiang B., Guo Z., Polystyrene Controlled Growth of Zerovalent Nanoiron/Magnetite on a Sponge-Like Carbon Matrix Towards Effective Cr(VI) Removal from Polluted Water, *RSC Adv.*, **6**: 110134-110145 (2016).